Differential cross sections at low energies for $^2H(d,p)^3H$ and $^2H(d,n)^3He$

Ronald E. Brown and Nelson Jarmie
Los Alamos National Laboratory, Los Alamos, New Mexico 87545
(Received 10 April 1989)

We have measured differential cross sections for the $^2H(d,p)^3H$ and $^2H(d,n)^3He$ reactions at 11 deuteron bombarding energies from 20 to 117 keV. The differential data are accurate to 2.0% (relative) over most of the energy range, with an additional scale error of 1.3%. Integrated cross sections are derived with total errors generally about 1.5%. The results are compared with other measurements and with an existing R-matrix analysis. We find a larger D-wave reaction amplitude than previously reported. Formulas for the cross sections and reactivities are given.

I. INTRODUCTION

The $^2H(d,p)^3H$ and $^2H(d,n)^3He$ reactions are of interest for the nuclear physics of few-nucleon systems, the compound nucleus ^4He being the lowest mass doubly magic system. The reactions are also of interest for fusion energy applications and for nuclear processes in the early solar system and early universe. The measurement techniques are based on those described in a previous publication[1] in which was presented a detailed study of the $^2H(t,\alpha)n$ reaction. The Los Alamos program in Low-Energy Fusion Cross Sections (LEFCS) was initiated in order to improve the accuracy and clear up discrepancies[2] in the basic fusion reactions, $^3H(d,\alpha)n$, $^2H(d,p)^3H$, $^2H(d,n)^3He$, and $^3H(t,\alpha)nn$. In particular, the existing data for the two $d+d$ reactions showed no major discrepancies, but it was clear that a significant improvement in accuracy would be beneficial. Knowledge of the rates for all of these reactions will be important in the design[3] of the first fusion reactors that are hoped eventually to provide sufficient energy for commercial use. These reactors are expected to operate over temperatures of $kT=1$–30 keV, which corresponds to lab bombarding energies near our range of 20–117 keV. Our $^3H(d,\alpha)n$ reaction study has been completed,[1,4,5] and data taking for the $^3H(t,\alpha)nn$ reaction is finished.

Many early cross-section measurements for the $^2H(d,p)^3H$ and $^2H(d,n)^3He$ reactions have been performed seeking improved absolute cross sections,[6–17] some because of a report of a narrow resonance near $E_d=100$ kev, and others to compare the two reaction branches for a study of charge symmetry. These older experiments (for a summary see Refs. 6, 18,and 19) did not verify the existence of a sharp resonance and were in general agreement with one another.

Spin-dependent experiments are necessary to determine uniquely the various partial wave contributions. This is especially important for the controversy[20–22] about the use of polarized deuteron beams in fusion reactors, a technique that was hoped to provide power with greatly reduced neutron production. More accurate cross-section data will also be of use in this analysis.

A recent and important cross-section experiment at low energy has been performed at Münster by Krauss, Becker, Trautvetter, Rolfs, and Brand,[23] whose measurements span the laboratory energy range of 6–325 keV. Also, new measurements are underway at Bruyères-le-Châtel,[24] France, and at the University of Giessen,[25] Germany.

The $d+d$ cross sections at low energy differ from those for $t+d$ in several respects. The $d+d$ cross sections are nonresonant, are several hundred times smaller than the $t+d$ cross section, and exhibit a marked angular anisotropy due to a significant amount of P-wave interaction.

We measured the $^2H(d,p)^3H$ and $^2H(d,n)^3He$ differential cross sections at 11 deuteron bombarding energies from 20 to 117 keV. The relative errors (standard deviations) in the differential cross sections are mostly about 2% and those in the integrated cross sections are about 0.8%. The scale error in both cases is 1.3%. These results greatly improve the accuracy over previous measurements, permitting us to obtain the most reliable low-temperature reactivities to date. Analytic forms for the cross sections and reactivities are provided and comparisons are made with R-matrix analyses. Preliminary reports of this work have been published.[26,27]

II. EXPERIMENT

Most details of the apparatus, data-taking procedure, and data-reduction techniques are given in Ref. 1. Figure 1 is a schematic diagram of the Los Alamos LEFCS facility. In brief, the experiment is performed by accelerating negatively charged deuterium ions through a windowless, cryogenically pumped, flowing gas target of deuterium and into a beam calorimeter. The charged reaction particles, p, t, and ^3He, are detected at six fixed angles (nominal lab angles of 45° left, 45° right, 75°, 90°, 120°, and 150°) with silicon surface-barrier detectors—neutrons are not detected. Table II of Ref. 1 contains detailed information on the exact angles and their relation to the beam. The mechanical angles are known to an accuracy of 0.03°, but the uncertainty of the actual beam direction raises the error in the laboratory angle to about 0.1°. The lab FWHM angular width of an individual detector is 3.2°. Because the cross sections vary rapidly with energy at the low energies of interest, an accurate determination of the beam energy in the reaction region of the gas target is

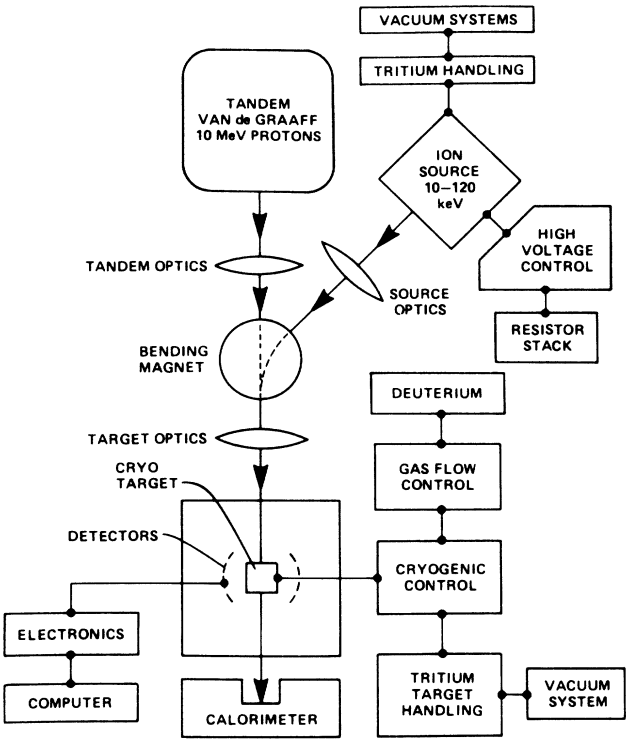

FIG. 1. Schematic diagram of the Los Alamos low-energy fusion cross-section facility (LEFCS).

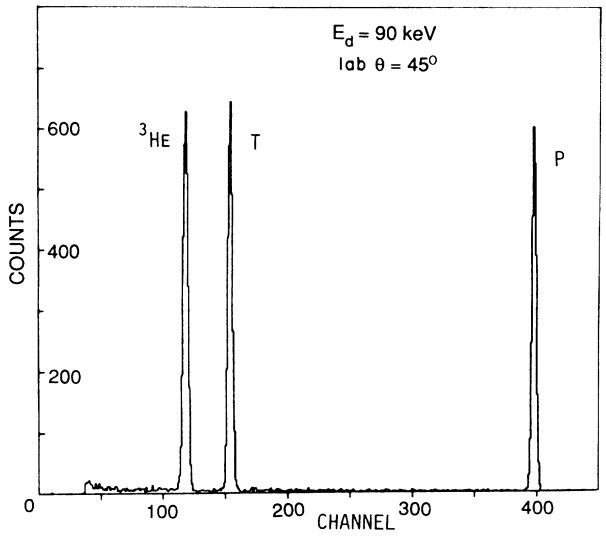

FIG. 2. The $d+d$ particle spectrum at 90 keV and 45° (lab). In order of increasing channel (energy) the peaks are for the particles ^{3}He, t, and p. Channel 400 corresponds to about 3.3 MeV.

mandatory. The ion accelerating potential is furnished by a high stability power supply and is measured with a 10^5:1 ratio resistive divider whose calibration is traceable to the National Bureau of Standards. The actual reaction energy will differ from the accelerating potential by small corrections arising from plasma potentials in the source duoplasmatron and energy loss in the gas target. The calorimeter (Fig. 1), which is used to determine the beam intensity, was calibrated to an accuracy of 0.1% by using the heat generated by a precision resistor embedded in it. The gas target density was determined by monitoring the target temperature and deuterium gas flow rate while bombarding the target with 10.04-MeV protons from the Los Alamos tandem Van de Graaff accelerator and detecting the elastically scattered protons. By using the absolute $p+d$ elastic cross section, which we had measured to 0.8% in a separate experiment at another experimental station, we were able to determine the deuterium density to 1.2%. Details of the procedure are given in Ref. 1.

Figure 2 shows a detected-particle spectrum at 45° for the $d+d$ reaction at 90 keV. The proton peak is at an energy ($\approx$3.3 meV) near that of the α particles in our ^{2}H$(t,\alpha)n$ experiment[1] and is in a region of very low background. The ^{3}He and triton peaks are at or below 1 MeV, and improvements had to be made by decreasing the electronic noise and neutron background before satisfactory results could be obtained. For example, the beam stop and various slits were baked to drive off impacted tritium from early triton-beam runs, thus eliminating background neutrons from the ^{3}H(d,n) reaction. An algorithm was installed in our data acquisition program to eliminate multiple noise events caused by occasional sparking at the extraction electrode of our accelerator. For the p^3H branch care had to be taken to account for the fact that at some beam energies true p-t coincidences could occur in a pair of left-right detectors.

III. RESULTS

A. Data reduction and errors

The methods of data reduction and error (standard deviation) determination are discussed in great detail in Ref. 1, and only certain aspects will be mentioned here. The relative error of the present data is dominated by counting statistics, background subtraction, and fluctuations in the target density. The absolute scale error is dominated by the uncertainty in the $p+d$ elastic calibration (1.2%). The relative errors in the differential cross sections are mostly about 2% except at the lowest energies where the error rises to 8–10%, all with a scale error of 1.3%. The total (absolute) error is the combination in quadrature of the relative and scale error. The relative errors (relative from energy to energy) in the integrated cross section are about 0.8%, except at the lowest energies where the error rises to 2.8% for the p^3H branch and 4.0% for the n^3He branch. Details are given in the tables. The deuteron bombarding energies are accurate to 15 eV, and the energy spread is about 40 eV (FWHM). The lab angular width is 3.2° (FWHM). The errors in the c.m. angle are about 0.1°. The angle and energy errors are transformed into cross-section errors.

As discussed in Ref. 1, it is useful for comparisons to convert the integrated cross sections to so called astrophysical S functions, which factors out from σ the energy

dependences of the de Broglie wavelength and the Coulomb penetrability. For reactions having a $d+d$ incident channel, S is given by

$$S=0.5\sigma E_d \exp(44.4021 E_d^{-1/2}) , \quad (1)$$

where σ is the integrated cross section in b (barns), E_d is the lab deuteron bombarding energy in keV, and S is expressed in keV b.

B. Angular distributions

A remarkable difference between the $d+d$ reaction and other nuclear fusion reactions is the large angular anisotropy present, even at these low energies. An example at 110 keV is given in Fig. 3. The anisotropy, which increases with increasing energy, is always larger for the n^3He branch.

We made measurements at six lab angles at each of 11 bombarding energies from 20 to 117 keV for each branch. Complete numerical tables of the differential cross sections are available from the authors and have also been deposited with the Physics Auxiliary Publication Service of the American Institute of Physics.[28]

The $d+d$ c.m. differential cross sections $\sigma(\theta)$ are symmetric about 90° because the target and beam particles are identical. We have analyzed $\sigma(\theta)$ by making a least-squares fit at each bombarding energy using the form $\sigma(\theta)=a+b\cos^2\theta+c\cos^4\theta$. With this three-term form

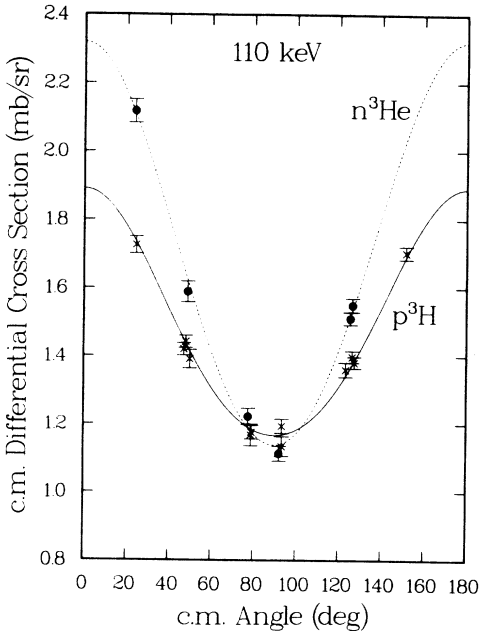

FIG. 3. The c.m. differential cross section $\sigma(\theta)$ for both branches of the $d+d$ reaction at a deuteron bombarding energy of 110 keV. The dashed line and solid circles are for the n^3He channel, and the solid curve and crosses are for the p^3H channel. Relative errors are shown. Note the suppressed zero. The curves are from a least-squares fit to the data of a function of the form $\sigma(\theta)=a+b\cos^2\theta+c\cos^4\theta$.

TABLE I. Coefficients a, b, and c from a least-squares fit to the differential cross section $\sigma(\theta)=a+b\cos^2\theta+c\cos^4\theta$ for the $d+d$ reactions. The relative error (standard deviation) in parenthesis corresponds to the last two digits of the value and is the square root of the diagonal element of the error matrix of the fit. The c coefficient for the lowest energies was set to zero. The lab deuteron energy E_d is accurate to ±15 eV.

^{2}H(d,p)^{3}H reaction			
E_d (keV)	a (mb/sr)	b (mb/sr)	c (mb/sr)
19.944	0.0208(10)	0.0023(22)	
29.935	0.0886(20)	0.0184(44)	
39.927	0.1882(28)	0.0659(62)	
49.922	0.3215(48)	0.076(27)	0.048(34)
59.917	0.4636(67)	0.168(38)	0.021(48)
69.914	0.6055(85)	0.251(44)	0.039(52)
79.912	0.7528(99)	0.250(52)	0.162(62)
89.911	0.8976(64)	0.378(32)	0.142(37)
99.909	1.041(12)	0.367(66)	0.276(80)
109.909	1.166(13)	0.521(69)	0.203(83)
116.909	1.243(21)	0.55(11)	0.34(12)
^{2}H($d,^3$He)n reaction			
E_d (keV)	a (mb/sr)	b (mb/sr)	c (mb/sr)
19.944	0.0181(14)	0.0108(31)	
29.935	0.0782(28)	0.0425(66)	
39.927	0.1780(39)	0.1027(91)	
49.922	0.2994(59)	0.212(14)	
59.917	0.4406(97)	0.303(55)	0.049(70)
69.914	0.564(10)	0.446(57)	0.111(73)
79.912	0.716(12)	0.537(68)	0.052(86)
89.911	0.8769(72)	0.674(41)	0.095(51)
99.909	1.018(16)	0.755(94)	0.20(12)
109.909	1.138(18)	1.09(10)	0.09(13)
116.909	1.231(25)	1.05(14)	0.20(17)

for $\sigma(\theta)$, the coefficients a and b generally will contain contributions from S, P, and D waves in the interaction and c will contain contributions from D waves only. At the lower energies in our range, the D-wave amplitude becomes small and it is reasonable to set it equal to zero. In that case the c coefficient is zero, the b coefficient contains contributions from P waves only, and the a coefficient contains contributions from both S and P waves. The values for the expansion coefficients a, b, and c from the fit are given in Table I. The errors stated in the table are the square roots of the diagonal elements of the error matrix of the fit and, therefore, do not reflect the correlations among the coefficients. The c coefficient is set to zero at the lowest energies where the D-wave amplitude is negligible.

C. Integrated cross sections and S functions

With the differential cross section in the form $\sigma(\theta)=a+b\cos^2\theta+c\cos^4\theta$, and with the coefficients a, b, and c determined from a least-squares fit to the data, we compute the angle-integrated cross section σ from $\sigma=4\pi(a+b/3+c/5)$. Values for σ and its error are given in Table II for the two branches. In computing the error, the full correlation among the coefficients is taken into account. The ^{2}H$(d,n)^3$He integrated cross section is given in the semilog plot of Fig. 4. Seen is the familiar steep slope from the Coulomb barrier penetration. Because of this rapid change of σ with E_d, it is more informative to give the results in the form of astrophysical S functions, as discussed above. Values of S and its error

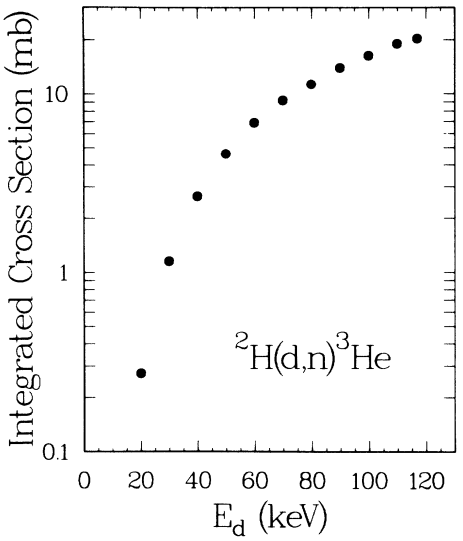

FIG. 4. Excitation function for ^{2}H$(d,n)^3$He integrated cross section σ. The total error bars are smaller than the plotting symbols.

TABLE II. Integrated cross section σ and astrophysical S function for the $d+d$ reactions. The relative error (standard deviation) is for both σ and S. The scale error is 1.3% for both branches. The lab deuteron energy E_d is accurate to ±15 eV. See the text for definition of S_a and S_b.

^{2}He$(d,p)^3$H reaction					
E_d (keV)	σ (mb)	S (keV b)	Rel. error (%)	S_a (keV b)	S_b (keV b)
19.944	0.2704	56.1	2.8	54.1	2.0
29.935	1.190	59.61	1.3	55.75	3.86
39.927	2.641	59.39	0.87	53.19	6.21
49.922	4.481	59.96	0.78	54.07	4.28
59.917	6.584	61.13	0.73	54.08	6.55
69.914	8.759	61.98	0.67	53.84	7.44
79.912	10.91	62.61	0.64	54.28	6.00
89.911	13.22	64.21	0.42	54.80	7.68
99.909	15.31	64.99	0.59	55.52	6.52
109.909	17.35	65.85	0.56	55.63	8.28
116.909	18.81	66.77	0.75	55.47	8.23
^{2}H$(d,n)^3$He reaction					
E_d (keV)	σ (mb)	S (keV b)	Rel. error (%)	S_a (keV b)	S_b (keV b)
19.944	0.273	56.7	4.0	47.27	9.42
29.935	1.161	58.1	1.8	49.23	8.91
39.927	2.667	59.99	1.2	50.31	9.67
49.922	4.651	62.24	1.0	50.35	11.89
59.917	6.927	64.31	1.0	51.41	11.77
69.914	9.237	65.36	0.86	50.18	13.21
79.912	11.38	65.32	0.82	51.65	12.92
89.911	14.08	68.41	0.46	53.53	13.71
99.909	16.44	69.79	0.79	54.29	13.42
109.909	19.10	72.50	0.75	54.27	17.36
116.990	20.36	72.27	0.89	54.90	15.61

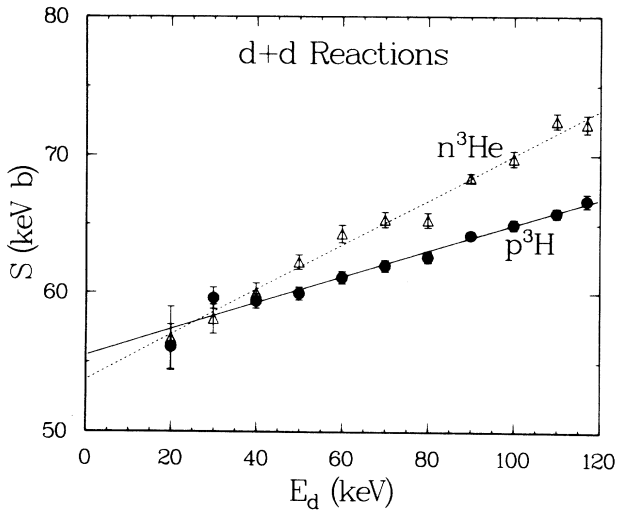

FIG. 5. The S function of Eq. (1) for both branches of the $d+d$ reactions vs deuteron bombarding energy. Note the suppressed zero. Relative errors are shown. The straight lines are from linear least-squares fits to the data.

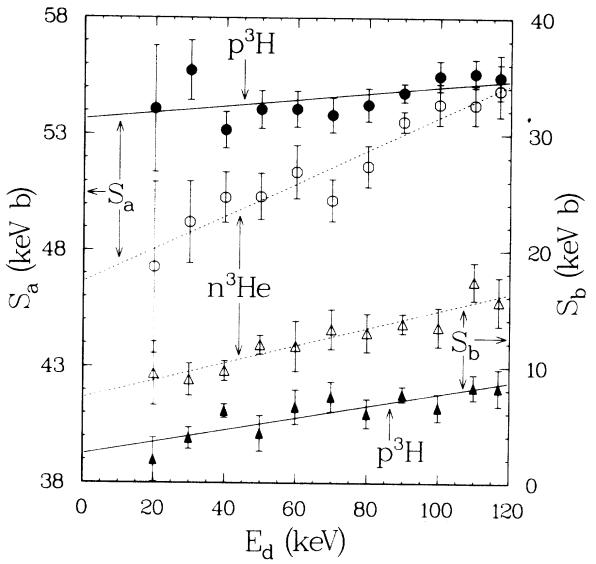

FIG. 6. Partial S functions S_a and S_b arising from the $4\pi a$ and $4\pi b/3$ contributions to the integrated cross section σ. Note the suppressed zero for S_a. The curves are linear least-squares fits to the data. Relative errors are shown.

are listed in Table II, and the S functions for the two channels are plotted in Fig. 5.

The curves in Fig. 5 show the results of linear, least-squares fits to S of the form $S=S_0(1+\alpha E_d)$. The fit coefficients and covariance matrix for both branches are given in Table III. The covariance matrix, sometimes called the error matrix, is defined as being twice the inverse of the matrix of second derivatives of χ^2 with respect to the fitting parameters, the derivatives being evaluated at the χ^2 minimum. Often the square root of the diagonal elements of the error matrix are quoted as the errors in the fitting parameters; however, that procedure does not take the correlations among the parameters into account, and therefore we have given the full error matrix for the fit.

Presented in Table II and in Fig. 6 are S_a and S_b, the astrophysical S functions for the a and b parts of the integrated cross section [i.e., the quantities $4\pi a$ and $4\pi b/3$ are treated as partial cross sections, and Eq. (1) is used to extract S_a and S_b]. At the lower energies where the D-wave contribution is small, S_b represents the P-wave contribution to S, and S_a contains both S and P waves.

IV. DISCUSSION

A. Angular shape and energy dependence

The low-energy $d+d$ reactions show an unusually large angular anisotropy. This stems from the dominance of negative-parity levels in the ^{4}He system ($E_x \approx 24$ MeV), allowing P waves to compete with S waves in spite of P-wave suppression by the angular momentum barrier. The main P-wave contribution at low energies is from a $J^\pi = 1^-$, $^3P_1$ state near the $d+d$ threshold.[29,30]

Less well understood are the different strengths of S (Fig. 5), the different strengths of S_b (Fig. 6), and the different slopes of S_a (Fig. 6) for the two channels. The S_a values do show a favoring of the p^3H branch at lower energies, as might be expected from an Oppenheimer-Phillips (O-P) mechanism.[31,32] The deuteron, easily electrically polarized, is expected to have an enhanced neutron stripping amplitude, favoring the p^3H branch, when the beam energy is well below the Coulomb barrier. A quantitative prediction of such an effect must take into

TABLE III. Linear fit coefficients and elements of the symmetric covariance matrix (error matrix) for the S function with its relative errors, where $S=S_0(1+\alpha E_d)$, with S and S_0 in keV b and E_d in keV. The fit variables are (1)$=S_0$ and (2)$=\alpha S_0$. Errors are given in parentheses for the least significant digits. For S_0 and αS_0 these are the square roots of the diagonal elements of the error matrix. For α these are computed by quadratic propagation from those for S_0 and αS_0 (the first quoted error) or by use of the full error matrix (the second quoted error).

		p^3H branch		n^3He branch	
S_0 (keV b)		55.49(46)		53.76(61)	
αS_0 (b)		0.094 82(540)		0.1623(72)	
α (keV^{-1})		0.001 709(98)(111)		0.003 019(138)(167)	
		(1)	(2)	(1)	(2)
covariance matrix	(1)	0.21034	$-0.237\,62\times10^{-2}$	0.367 87	$-0.419\,52\times10^{-2}$
	(2)	$-0.237\,62\times10^{-2}$	$0.291\,84\times10^{-4}$	$-0.419\,52\times10^{-2}$	$0.518\,78\times10^{-4}$

account the identity of the target and projectile, the steepness in energy of the cross section, and the amount of isospin mixing: probably large in this case, as there are nearby, broad $T=1$ and $T=0$ levels in the ^{4}He system.[29] The difficulties are demonstrated by Cecil, Peterson, and Kunz,[33] who have made a DWBA calculation for the system ^{6}Li(d,n) and ^{6}Li(d,p), also a mirror system, at bombarding energies from 60 to 160 keV. The calculation predicts an *O-P* effect that greatly overestimates the experimental results. In our case, even though S_a favors the p^3H branch, the larger values of S_b for the n^3He branch (Fig. 6) result in an overall larger reaction rate (S in Fig. 5) for that branch, and therefore, we did not attempt any such O-P calculations. The energy variations of the S functions seen in Figs. 5–8 are influenced by an increasing angular momentum barrier and decreasing effect of nearby broad resonances as the energy is lowered.

B. Integrated cross-section comparison

Comparison of our integrated cross-section data with others is shown in Figs. 7 and 8. Total errors are shown. The solid circles are the present Los Alamos data, the crosses are the Münster data of Krauss *et al.*,[23] and the squares are a representative selection of the large amount of data from other experiments that measured absolute cross sections.[6–17] The curve is from an R-matrix analysis of the mass-4 system[29,34] that does not include the present data or the Münster results. No evidence for a sharp resonance is seen, confirming the older experiments, and the bulk of the older data with their larger errors are in agreement with our data. The Münster cross sections are 5–10% lower than our measurements, but

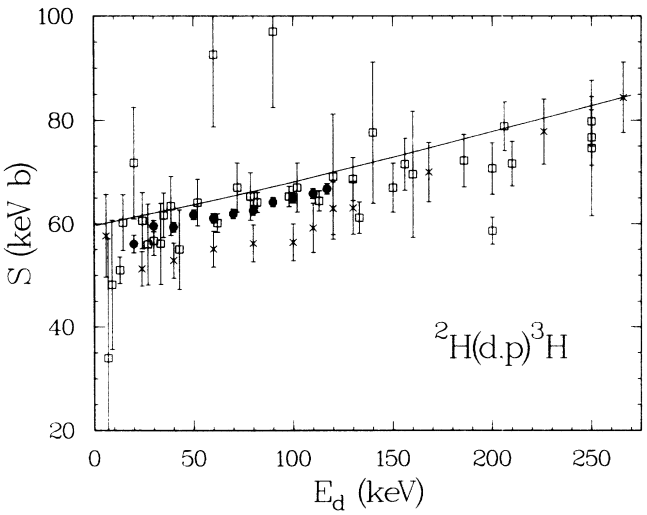

FIG. 7. The S function of Eq. (1) for the ^{2}H$(d,p)^3$H reaction as a function of deuteron bombarding energy. Total errors are shown. The solid circles are the present Los Alamos data. The crosses are from the Münster data (Ref. 23). The squares are a representative selection of data from other experiments (Refs. 6–17). The curve is from a unified, mass-4, R-matrix analysis (Refs. 29, 34, 43) that does not include the Los Alamos or Münster data. Note the suppressed zero.

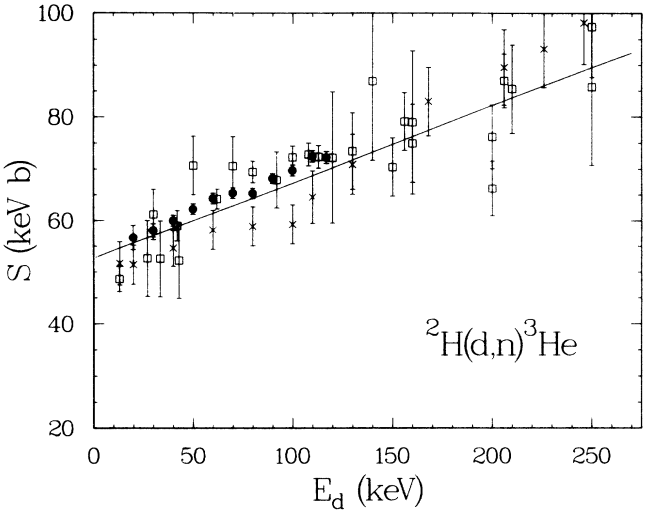

FIG. 8. The S function of Eq. (1) for the ^{2}H$(d,n)^3$He reaction as a function of deuteron bombarding energy. Total errors are shown. The solid circles are the present Los Alamos data. The crosses are from the Münster data (Ref. 23). The squares are a representative selection of data from other experiments (Refs. 6–17). The curve is from a unified, mass-4, R-matrix analysis (Refs. 29, 34, 43) that does not include the Los Alamos or Münster data. Note the suppressed zero.

are in fairly good agreement with us considering that their absolute error is 6–8%. Their measurements extend up to 325-keV deuteron energy. While we feel confident that their data below 117 keV should be normalized to our more accurate measurements, it is not clear what should be recommended concerning their higher-energy data in the light of possible energy related systematic errors, especially since they used different experimental facilities for the lower and higher energies.

C. Extrapolation to astrophysical energies

In the past, there has been considerable effort[18,35–37] to find a meanignful way of extrapolation of the integrated cross section to very low energies. By inspection of Figs. 5, 7, and 8, it is clear that use of the astrophysical S function greatly simplifies the task, especially when no sharp resonances in the cross section are nearby and the S functions are slowly varying with energy. Using the least-squares fit of our data in Sec. III C, we find the zero-energy intercepts S_0 that are given in Table III. By combining the 1.3% scale error with the relative errors in Table III we find the total error in these intercepts to be $\pm 1.5\%$ for the p^3H branch and $\pm 1.7\%$ for the n^3He branch. An R-matrix fit using our data is expected to give similar results for S_0.

D. Theoretical review

Fick and Weiss published[18] in 1973 a summary of the significant theory to that date. (See also Refs. 19 and 30 for a general summary of measurements and theory to 1973.) They reviewed and improved the early work of Konopinski, Teller, and others,[38] who explained, with a

simple type of R-Matrix theory, the general shape of the excitation function of the integrated cross section primarily as the result of barrier penetration. Fick and Weiss showed that the "direct reaction" approach of Boersma[39] and others[40,41] was formally equivalent to these early R-Matrix calculations. They also pointed out that when only S and P waves were considered, three energy- and model-independent parameters were necessary for a successful phenomenological fit to the cross-section data known up to 1973, although those parameters were only poorly determined by that data. They noted that P-wave contributions are significant even at the lowest energies, which results in the anisotropy of the differential cross section remaining nonzero even as zero energy is approached. Therefore, quantities that represent the anisotropy should *not* be extrapolated to zero at zero energy, as was incorrectly shown in Figs. 7 and 9 of Ref. 6. Remaining unexplained was the fact that the P-wave contribution to the cross section was several times greater for the n^3He channel than for the p^3H channel. It was also not clear that the fits they carried out lead to an improved understanding of the character of the ^{4}He compound nucleus other than that the low-energy $d+d$ region is dominated by negative parity states.

Since 1973 there have been a number of improved experiments and theoretical[21] papers. The new cross sections measured in the present experiment at Los Alamos and at Münster[23] have already been discussed. Several spin-dependent measurements have been done or are in progress.[22,25]

Theoretical calculations for these reactions are available using the Resonating Group Method (RGM).[20,42] The RGM predictions reproduce the general trend of the data fairly well and could be considered a reasonable fit when the purity of the physical assumptions and the lack of arbitrary variables are taken into account. However, when looked at in detail, the accuracy of our data remains a challenge to the RGM calculations.

The R-matrix work of G. M. Hale and his collaborators[29,34,43,44] provides the best parametrization of all the data channels for the mass-4 system (up to ~29 MeV excitation in ^{4}He, or 10-MeV deuteron bombarding energy) and, in addition, provides information about the energy levels of ^{4}He. The results of R-matrix fits[43] that do not include the present data are compared with our data in Secs. IV B, IV D, and in Figs. 7–10.

Hale finds with an improved R-Matrix fit[44] that uses our new data and recent spin-dependent measurements,[25] that charge symmetry between the two channels holds if proper account is taken of isospin mixing[34,45] by the Coulomb interaction in the internal nuclear region. This conclusion supports experiments[46] at higher energies that also found no charge-symmetry violation, in contrast to some earlier work (referred to in Ref. 46). The internal-Coulomb effect is quite significant in fitting cross sections and spin-dependent data.[34,44]

Recently, Hale has developed a computer code that finds the poles and residues of the S matrix from a set of R-matrix parameters. One motivation for doing this is that it is not always easy to interpret the parameters of the R matrix in terms of the level structure of the compound system, especially in a complicated multilevel analysis. Therefore it is often better to extract resonance parameters from an asymptotic quantity, such as the S matrix. This technique has been applied to an analysis of the ^{2}H$(t,\alpha)n$ reaction[4,5] in which the low-energy, $3/2^+$ resonance in ^{5}He was studied. The structure of ^{4}He may be able to be studied in a similar way.

E. Anisotropies and D-wave strength

In Figs. 9 and 10 we show the angular anisotropies, $[\sigma(0°)-\sigma(90°)]/\sigma(90°)$, which can be expressed in terms of our expansion coefficients as $(b+c)/a$. There we compare our results with those of Theus *et al.*,[6] the Münster work,[23] and an R-matrix fit[29,34,43] that does not include our (or the Münster) data. We noticed that Table 1 of Theus *et al.*[6] does not transform properly into their Table 2. We learned from the authors[6] that there had been a computational error and that their Tables 2 and 3 (derived from Table 2) are incorrect. We base our discussion below on the assumption that the coefficients and errors in Table I of Ref. 6 are correct.

In Figs. 9 and 10, we note again that the n^3He anisotropy is considerably larger than that of the p^3H branch (as can also be seen in Fig. 3). In evaluating the anisotropies, the results of Theus *et al.* perhaps should be given the greatest weight, since they measured $\sigma(\theta)$ at more angles, both above and below 90°, than was done in the other experiments, thereby obtaining smaller errors for the anisotropies. We stress that the *absolute* cross sections from our work are the most accurate yet measured, as is shown in Figs. 7 and 8.

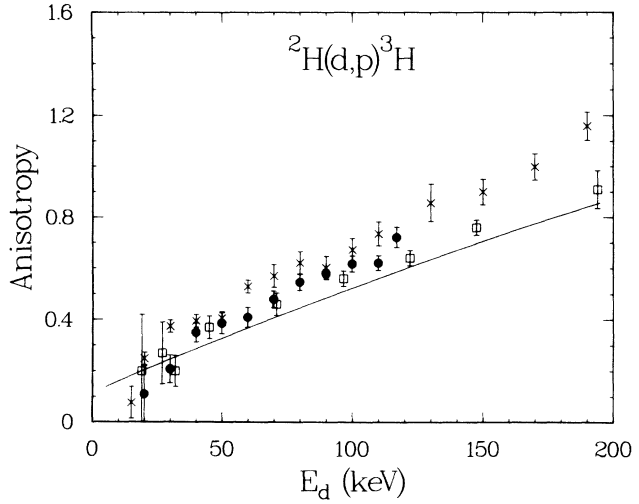

FIG. 9. ^{2}H$(d,p)^3$H angular anisotropy $[\sigma(0°)-\sigma(90°)]/\sigma(90°)$ vs deuteron bombarding energy. The solid circles are the present data, the squares are the data of Theus *et al.* (Ref. 6) and the crosses show the data from Münster (Ref. 23). The curve is from a unified, mass-4, R-matrix analysis (Refs. 29, 34, 43) that does not include the present or the Münster data. The curve has a nonzero intercept at zero energy.

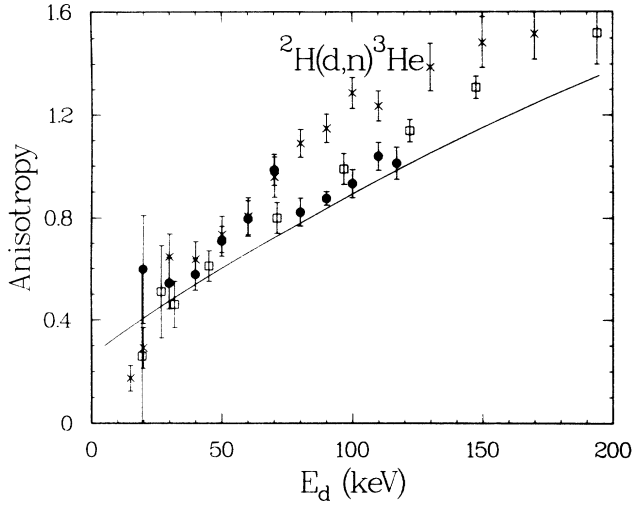

FIG. 10. ^{2}H$(d,n)^3$He angular anisotropy $[\sigma(0°)-\sigma(90°)]/\sigma(90°)$ vs deuteron bombarding energy. The solid circles are the present data, the squares are the data of Theus *et al.* (Ref. 6) and the crosses show the data from Münster (Ref. 23). The curve is from a unified, mass-4, *R*-matrix analysis (Refs. 29, 34, 43) that does not include the present or the Münster data. The curve has a nonzero intercept at zero energy.

We computed the Münster[23] anisotropies from Table 1 of Ref. 23. For the p^3H branch (Fig. 9) they are in fairly good agreement with our results and those of Theus *et al.*,[6] with a tendency to be one or two standard deviations higher, especially at the larger energies. For the n^3He branch (Fig. 10) below about 80 kev, they are in good agreement with our results and those of Theus *et al.*[6] At the higher energies their anisotropies increase more rapidly, becoming 2 to 4 standard deviations higher. We notice in Fig. 9 of their paper that, in the angular distribution example at 270 keV, they obtained very little data below 90° (c.m.), and in the 50-keV example their Legendre analysis is a poor fit to their data. Generally, the Münster results, both *S* functions and anisotropies, tend to increase at a more rapid rate as the energy rises than do the present results.

In our analysis we have found a larger *D*-wave reaction amplitude than one would expect from previous work. For example, in Table IV we list the ratio c/a at 100 keV, where the *D*-wave contribution is small but significant. We compare our results with those of Münster,[23] Theus *et al.*,[6] and the above mentioned *R*-matrix analysis.[29,34,43] Considering only the Los Alamos data, the indication would be that the level-structure used in the *R*-matrix analysis did not provide sufficient *D*-wave strength, which comes from the tails of *D*-wave levels higher in excitation in the ^{4}He compound system. Notice, however, the Theus c/a for the p^3H branch agrees with Hale, but not with us. Little more can be said because of the large errors on the rest of the values.

A calculation was made by Bevelacqua[47] using an *R*-matrix approach modified by DWBA terms to account for basis-state limitations. His results stressed the need for *D* waves, and he finds a small but significant *D*-wave contribution beginning around 70 keV and rising with energy. This agrees reasonably well with our result, which finds the need for a *D*-wave contribution beginning at 50 to 60 keV.

TABLE IV. The c/a coefficient ratio at $E_d=100$ keV. The relative standard deviations in parentheses are in the last digits of the c/a values.

	p^3H branch	n^3He branch	Reference
Los Alamos	0.27(08)	0.19(12)	Present work
Münster	0.16(10)	0.06(12)	23
Theus	0.04(02)	0.12(03)	6
R-matrix	0.046(003)	0.044(005)	29,34,43

V. ANALYTIC FORMULAS FOR THE CROSS SECTION AND REACTIVITY

The linear least-squares fit of the *S* functions of Table II to the form $S=S_0(1+\alpha E_d)$ produces values for S_0 and α for the two branches as given in Table III. By using Eq. (1) we may express the integrated cross section σ in the form

$$\sigma=2S_0(1+\alpha E_d)E_d^{-1}\exp[-(44.4021E_d^{-1/2})] , \quad (2)$$

where E_d is the deuteron bombarding energy in keV, σ is in b (barns), and S_0 (in keV b) and α are given in Table III for each channel.

In a deuterium plasma the Maxwellian reactivity $\langle\sigma v\rangle$ in cm^3/sec at a temperature kT (keV) is given by

$$\langle\sigma v\rangle=7.20458\times10^{-19}S_{\rm eff}\tau^2e^{-\tau} , \quad (3)$$

where $\tau=18.808(kT)^{-1/3}$, $S_{\rm eff}=S_0\{1+[5/(12\tau)]+2\alpha[E_0+(35/36)kT]\}$ (keV b), and $E_0=6.2696\ (kT)^{2/3}$ (keV). S_0 (in keV b) and α are given in Table III for each reaction channel, and E_d is the deuteron bombarding energy in keV. Details about these formulas and their derivation are given in Sec. V B of Ref. 1 and in the references given there. A beam-target reactivity (as different from the Maxwellian-plasma reactivity calculation above) using the present data has been made by Mikkelsen.[48] Further information on reactivity calculations can be found in the references of Mikkelsen's paper, in Sec. V B of Ref. 1, in the references in McNally *et al.*[49] and in the papers of Haubold[50] and his collaborators.

The range of temperature over which Eq. (3) is valid depends on to how high an energy E_d the linear fit to *S* (Fig. 5 and Table III) for our data gives a reasonably accurate representation of an extended data set, such as depicted in Figs. 7 and 8. For example, if one considers the range of validity of the fit to end at our highest energy, $E_d=120$ keV (Fig. 5), then, by inspecting the integrand of the reactivity integral, Eq. (3) would be applicable only

in the range $kT=0$–6 keV. However, by inspecting Figs. 5, 7, 8, and Ref. 23, one can draw the conclusion that the fit of Table III is quite reasonable up to as high a lab energy as 300 keV. We therefore propose that Eq. (3) can be applied up to a kT value of about 18 keV.

The above formulas (and our data) are not corrected for screening by the electrons bound to the molecules of the target gas, an effect which eventually must become important as the energy is decreased. In Sec. VI of Ref 1 we made a rough estimate and found that a change in the cross section at our lowest energy was smaller than the error and was not significant. More recent and detailed screening calculations[51,52,53] have been done. They indicate that the corrections may be larger than we had estimated and that the "bare-nucleus" cross section could be smaller than our present data at the lower energies. We leave to the user of our data the determination of any such corrections for his particular reaction environment and have not included shielding corrections in this paper.

VI. CONCLUSIONS

We have measured differential cross sections for the ^{2}H$(d,p)^3$H and ^{2}H$(d,n)^3$He reactions at 11 deuteron bombarding energies from 20 to 117 keV. The differential data are accurate to 2.0% over most of the energy range, with a scale error of 1.3%. Integrated cross sections are derived with total errors generally about 1.5%. This absolute accuracy represents a marked improvement over the accuracy of previous experiments. We present analytic formulas for the cross section and reactivity, which should be of practical use in general fusion-reactor design, in the possible use of polarized-deuteron injection in future fusion-reactors,[20–22] and in considering other methods of energy production. The primary theoretical use, at this time, will be to help determine the energy levels of ^{4}He by improving fits to the mass-4 system with powerful R-matrix programs.[29,34,43,44] This, in turn, could influence RGM[20,42,54] calculations. The cross sections at very low energies, as specified in Table III, will be of interest to astrophysics. A powerful phenomenological tool such as the energy-dependent R-matrix technique is needed to tie together the various experiments in different channels and provide the best fit. New data from the French[24] and German[25] groups would be valuable in this respect and, hopefully, would shed light on the discrepancies noted in this paper, in particular, the anisotropy and the D-wave strength. We urge future experimenters to make their angular distribution measurements as accurate as possible.

ACKNOWLEDGMENTS

We wish to thank R. Martinez for his loyal and effective help in all phases of operating the experiment. We are grateful to G. M. Hale for valuable discussions concerning the R-matrix analyses and the physics of the mass-4 system. We appreciate our discussions with F. E. Cecil, R. J. Peterson, L. M. Hively, L. A. Beach, and R. Feldbacher. R. A. Hardekopf, J. Ross, M. S. Peacock, and the Los Alamos Ion Beam Facility staff were all very helpful in many ways.

[1]N. Jarmie, R. E. Brown, and R. A. Hardekopf, Phys. Rev. C **29**, 2031 (1984); **33**, 385 (1986).

[2]N. Jarmie, Nucl. Sci. Eng. **78**, 404 (1981); Los Alamos National Laboratory Report No. LA-8087 (1980).

[3]N. Jarmie, in Proceedings of the Advisory Group Meeting on Nuclear Data for Fusion Reactor Technology, Gaussig/Dresden, 1986 [International Atomic Energy Agency, Report No. TECDOC 457, 1988], p. 79.

[4]R. E. Brown, N. Jarmie, and G. M. Hale, Phys. Rev. C **35**, 1999 (1987); **36**, 1220 (1987).

[5]G. M. Hale, R. E. Brown, and N. Jarmie, Phys. Rev. Lett. **59**, 763 (1987); D. Morgan and M. R. Pennington, *ibid.* **59**, 2818 (1987); G. M. Hale, R. E. Brown, and N. Jarmie, *ibid.* **59**, 2819 (1987).

[6]R. B. Theus, W. I. McGarry, and L. A. Beach, Nucl. Phys. **80**, 273 (1966); L. A. Beach and R. B. Theus (private communication); see Sec. IV E for an important statement on the accuracy of the data tables of this reference.

[7]K. G. McNeill and G. M. Keyser, Phys. Rev. **81**, 602 (1951).

[8]W. A. Wenzel and W. Whaling, Phys. rev. **88**, 1149 (1952).

[9]P. A. Davenport, T. O. Jeffries, M. E. Owen, F. V. Price, and D. Roaf, Proc. R. Soc. London, Ser. A **216**, 66 (1953).

[10]E. A. Eliot, D. Roaf, and P. F. D. Shaw, Proc. R. Soc. London, Ser. A **216**, 57 (1953).

[11]G. Preston, P. F. D. Shaw, and S. A. Young, Proc. R. Soc. London, Ser. A **226**, 206 (1954).

[12]D. Magnac-Valette, E. LaCombe, R. Bilwes, and P. Cüer, J. Phys. Radium **21**, 125 (1960).

[13]A. Von Engel and C. C. Goodyear, Proc. R. Soc. London, Ser. A **264**, 445 (1961).

[14]K. G. McNeill, Philos. Mag. **46**, 800 (1955).

[15]V. A. Davidenko, A. M. Kucher, I. S. Pogrebov, and IU. F. Tuturov, At. Energ. (Eng. Trans.) Suppl. **5**, 7 (1957).

[16]A. S. Ganeev, A. M. Govorov, G. M. Osetinskii, A. N. Rakivnenko, I. V. Sisov, and V. S. Siksin, At. Energ. (Eng. Trans.) Suppl. **5**, 21 (1957).

[17]W. R. Arnold, J. A. Phillips, G. A. Sawyer, E. J. Stovall, Jr., and J. L. Tuck, Phys. Rev. **93**, 483 (1954); Los Alamos Scientific Laboratory Report No. LA-1479 (1953).

[18]D. Fick and U. Wiess, Z. Phys. **265**, 87 (1973), and references therein.

[19]G. Pospiech, H. Genz, E. H. Marlinghaus, A. Richter, and G. Schrieder, Nucl. Phys. **A239**, 125 (1975).

[20]H. M. Hofmann, G. M. Hale, and R. Wölker, in *Proceedings of Few Body Approaches to Nuclear Reactions in Tandem and Cyclotron Energy Regions, Tokyo, 1986,* edited by S. Oryu and T. Sawada (World Scientific, Singapore, 1987), p. 162 and references therein.

[21]S. Abu-Kamar, M. Igarashi, R. C. Johnson, and J. A. Tostevin, J. Phys. G **14**, L1 (1988), and references therein.

[22]J. S. Zhang, K. F. Liu, and G. W. Shuy, Phys. Rev. Lett. **57**, 1410 (1986), and references therein.

[23]A. Krauss, H. W. Becker, H. P. Trautvetter, C. Rolfs, and K. Brand, Nucl. Phys. **A465**, 150 (1987).
[24]G. Haouat (private communication).
[25]E. Pfaff and G. Clausnitzer (private communication).
[26]N. Jarmie and R. E. Brown, Nucl. Instrum. Methods **B10/11**, 405 (1985).
[27]R. E. Brown and N. Jarmie, Radiat. Eff. **92**, 45 (1986); in *Proceedings of the International Conference on Nuclear Data for Basic and Applied Science, Santa Fe, 1985,* edited by P. G. Young, R. E. Brown, G. F. Auchampaugh, P. W. Lisowski, and L. Stewart (Gordon and Breach, New York, 1986), p. 45.
[28]See AIP document no. PAPS PRVCA-41-1391-14 for 14 pages of our numeical c.m. differential cross-sections with errors and associated information. Order by PAPS number and journal reference from American Institute of Physics, Physics Auxiliary Publication Service, 335 East 45th Street, New York, NY 10017. The price is $1.50 for each microfiche (up to 98 pages) or $5.00 for photocopies of up to 30 pages, and $0.15 for each additional page over 30 pages. Make checks payable to the American Institute of Physics.
[29]G. M. Hale and D. C. Dodder, in *Proceedings of the Conference on Few Body Problems in Physics, Karlsruhe, 1983,* edited by B. Zeitnitz (Elsevier, Amsterdam, 1984), Vol. II, p. 433; see also Nucl. Phys. **A416**, 363c (1984), and private communication.
[30]S. Fiarman and W. E. Meyerhof, Nucl. Phys. **A206**, 1 (1973).
[31]E. O. Lawrence, E. McMillan, and R. L. Thornton, Phys. Rev. **48**, 493 (1935).
[32]J. R. Oppenheimer and M. Phillips, Phys. Rev. **48**, 500 (1935).
[33]F. E. Cecil, R. J. Peterson, and P. D. Kunz, Nucl. Phys. **A441**, 477 (1985).
[34]G. M. Hale and D. C. Dodder, in *Nuclear Cross Sections for Technology,* Natl. Bur. Stand. (U.S.) Spec. Publ. No. 594, edited by J. L. Fowler, C. H. Johnson, and C. D. Bowman (U.S. GPO, Washington, D.C., 1980), p. 650.
[35]J. N. Bahcall, Astrophys. J. **143**, 259 (1966).
[36]J. E. Monahan, A. J. Elwyn, and F. J. D. Serduke, Nucl. Phys. **A269**, 61 (1976).
[37]J. G. Brennan, Phys. Rev. **111**, 1592 (1958).
[38]E. J. Konopinski and E. Teller, Phys. Rev. **73**, 822 (1948); F. M. Beiduck, J. R. Pruett, and E. J. Konopinski, Phys. Rev. **77**, 622 (1950); and **77**, 628 (1950), references therein.
[39]H. J. Boersma, Nucl. Phys. **A135**, 609 (1969).
[40]J. C. Duder, H. F. Glavish, and R. Ratcliff, in *Proceedings of the Third International Symposium on Polarization Phenomena in Nuclear Reactions, Madison, 1970,* edited by H. H. Barschall and W. Haeberli (University of Wisconsin Press, Madison, 1971), p. 459.
[41]D. U. L. Yu, Prog. Theor. Phys. **36**, 734 (1966).
[42]H. Kanada, T. Kaneko, and Y. C. Tang, Phys. Rev. C **34**, 22 (1986).
[43]G. M. Hale, Trans. Am. Nucl. Soc. **46**, 269 (1984).
[44]G. M. Hale and D. C. Dodder, Bull. Am. Phys. Soc. **33**, 1571 (1988).
[45]V. A. Sergeyev, Phys. Lett. **38B**, 286 (1972).
[46]R. A. Hardekopf, R. L. Walter, and T. B. Clegg, Phys. Rev. Lett. **28**, 760 (1972).
[47]J. J. Bevelacqua, J. Phys. G **7**, 1255 (1981).
[48]D. R. Mikkelsen, Princeton Plasma Physics Laboratory Report PPPL-2566 (1988); Nucl. Fusion **29**, 1113 (1989).
[49]J. Rand McNally, Jr., K. E. Rothe, and R. D. Sharp, Oak Ridge National Laboratory Report No. ORNL/TM-6914 (1979).
[50]H. J. Haubold, and A. M. Mathai, J. Math. Phys. (N.Y.) **27**, 2203 (1986); Ann. Phys. (Leipzig) **41**, 380 (1984), and the references in these two papers.
[51]H. J. Assenbaum, K. Langanke, and C. Rolfs, Z. Phys. A **327**, 461 (1987).
[52]S. Engstler, A. Krauss, K. Neldner, C. Rolfs, U. Schröder, and K. Langanke, Phys. Lett. B **202**, 179 (1988).
[53]K. Langanke and C. Rolfs, Mod. Phys. Lett. **A4**, 2101 (1989); also private communication.
[54]H. M. Hofmann, Nucl. Phys. **A416**, 363c (1984).